JOURNAL

OF THE AMERICAN CHEMICAL SOCIETY

VOLUME 110, NUMBER 25 DECEMBER 7, 1988

The Use of Lanthanides for Solution Structure Determination of Biomolecules by NMR: Evaluation of the Methodology with EDTA Derivatives as Model Systems

Marvin D. Kemple,*,[†] Bruce D. Ray,[†] Kenny B. Lipkowitz,[‡] Franklyn G. Prendergast,[§] and B. D. Nageswara Rao[†]

Contribution from the Departments of Physics and Chemistry, Indiana University—Purdue University at Indianapolis, 1125 East 38th Street, P. O. Box 647, Indianapolis, Indiana 46223, and the Department of Biochemistry and Molecular Biology, Mayo Foundation, Rochester, Minnesota 55905. *Received October 30, 1987*

Abstract: The methodology of using lanthanide ions to obtain structures of biological macromolecules in liquid solution from proton NMR measurements was critically examined with indole-EDTA and benzyl-EDTA as model systems. Both of these molecules form tight monodentate complexes with lanthanide ions. Shifts of proton resonance frequencies induced by the binding of Pr^{3+}, Nd^{3+}, Eu^{3+}, and Yb^{3+} (LIS) were measured at 5-deg intervals from 5 to 60 °C at a frequency of 300 MHz. Enhancements of proton spin-lattice relaxation rates, T_1^{-1}, and line widths due to the ion binding (LIR) were measured at 30 °C at frequencies of 200, 300, and 470 MHz. La^{3+} and Lu^{3+} served as diamagnetic references. Structures of these molecules determined from molecular mechanics calculations formed a basis for analysis of the NMR data. Those structures along with 2D-COSY and proton decoupling experiments were combined to assign the proton resonances which were all in slow exchange. A method of analysis of the LIS utilizing linear least-squares fitting of the data to expressions involving elements of the magnetic susceptibility tensors of the ions is given. Theoretical values for the magnetic properties of the ions were not used to separate the contact (through bond) and pseudocontact (through space) contributions to the LIS. The contact shifts were included as fitting parameters. The temperature dependence of the LIS was of no use in making assignments or in separating the contact and pseudocontact shifts; it was only useful for unraveling overlapping resonances. The results showed differences in the orientation of the principal axes of the magnetic susceptibility tensors of the ions within the same molecule as well as deviations of the orientations from the "near"-symmetry directions of the molecules. Furthermore, the magnetic susceptibility tensors deviated greatly from axial symmetry with asymmetry parameters ranging from 0.09 to 0.97. For Yb^{3+}, LIS analysis was not feasible because unresolved scalar couplings precluded the making of complete assignments. In general, the LIR yielded reasonable values for the ratios of distances of the protons from the ion. In order to determine detailed molecular structure from these kinds of measurements the coordinates of at least five paramagnetic nuclei in the molecule must be known from other sources. LIR and LIS values, the latter obtained with at least two different ions, are essential to establish distance and orientation, respectively.

I. Introduction

Nuclear magnetic resonance (NMR) has become a versatile and powerful method for ascertaining the structure of molecules in liquid solution especially since, in contrast to X-ray methods, NMR is extremely sensitive to proton placement. Among those NMR techniques is the subject of the study described here, viz., the interpretation of the effects of paramagnetic lanthanide ions on the NMR parameters of nuclei in molecules, to which the ion is bound or proximate, in terms of the geometry of the molecule. Because of their spectroscopic properties lanthanide ions have been broadly used as presumed isomorphous replacements for Ca^{2+} in biological systems.[1-4] The lanthanides apparently bind at calcium sites on proteins and smaller molecules as well, but their ability to trigger the same biological response as calcium is not predictable. Paramagnetic lanthanide ions have been used to advantage as structural probes of calcium binding proteins by Lee and Sykes[5-7] in studies of carp parvalbumin by NMR.

The binding of a particular paramagnetic lanthanide ion by a molecule can cause two types of effects. The first of these, increases in nuclear spin-lattice relaxation rates (T_1^{-1}) and

---

* To whom reprint requests should be addressed.

[†] Department of Physics, Indiana University—Purdue University at Indianapolis.

[‡] Department of Chemistry, Indiana University—Purdue University at Indianapolis.

[§] Mayo Foundation.

(1) Brittain, H. G.; Richardson, F. S.; Martin, R. B. *J. Am. Chem. Soc.* **1976**, *98*, 8255–8260.

(2) Martin, R. B.; Richardson, F. S. *Q. Rev. Biophys.* **1979**, *12*, 181–209.

(3) Horrocks, W. DeW., Jr. *Advances in Inorganic Biochemistry*; Eichhorn, G. L., Marzilli, L. G., Eds.; Elsevier: New York, 1982; pp 201–261.

(4) Evans, C. H. *Trends Biochem. Sci.* **1983**, *8*, 445–449.

(5) Lee, L.; Sykes, B. D. *Biophys. J.* **1980**, *32*, 193–210.

(6) Lee, L.; Sykes, B. D. *Biochemistry* **1980**, *19*, 3208–3214.

(7) Lee, L.; Sykes, B. D. *Biochemistry* **1983**, *22*, 4366–4373.

0002-7863/88/1510-8275$01.50/0

spin–spin relaxation rates (T_2^{-1}) referred to as lanthanide-induced relaxation (LIR), depends on the inverse sixth power of the distance between the ion and the nucleus[8,9] in question. LIR is independent of orientation. The binding of the paramagnetic ion can also induce frequency shifts[10] in the NMR spectrum of the molecule relative to that for a complex with a diamagnetic ion. These lanthanide-induced shifts (LIS) have two contributions, (i) the Fermi contact shift[10,11] and (ii) the pseudocontact or dipolar shift.[10,12] Orientational information is available only from the pseudocontact shift, which will be nonzero in liquid solution only if the magnetic susceptibility of the bound paramagnetic ion is anisotropic. This shift depends on the inverse cube of the distance between the ion and the nucleus as well as on the orientation of the ion–nucleus vector relative to the principal axes of the susceptibility tensor.

To obtain complete geometrical information for the molecule from this method, a general procedure must be followed. (1) The resonances observed in the spectrum of the ion–molecule complex are assigned to specific nuclei. (2) Elements of the magnetic susceptibility tensors of the ions are determined from the LIS based upon the independently known coordinates of some of the nuclei in the molecule. (A key to this step and the fourth step below is a valid separation of the contact and pseudocontact contributions to the LIS.) (3) The distances from the ion to the remaining nuclei are calculated from the LIR. (4) The two angular coordinates for each of these nuclei are determined from LIS data with two or more ions. All of the four steps are fraught with assumptions and operational problems. No consensus exists in the literature[13–24] concerning the optimum manner to address these difficulties in order to obtain reliable structural information.

The problem of assignment of resonances is straightforward if the resonances are in fast exchange since a single resonance is observed at the concentration-weighted average of the line positions with and without the paramagnetic ion bound. The LIS is then obtained by extrapolating a titration of this resonance position to infinite paramagnetic ion concentration. On the other hand, if slow exchange prevails as it does for the molecules in this study, separate resonances for a given nucleus are observed for each complex. The fully paramagnetically shifted resonance positions are observed in the spectrum, but the assignment of those resonances becomes extremely difficult. This question is addressed below with special reference to the reliability of using the temperature dependence of the paramagnetically shifted resonances for making such assignments. Given the avidity with which lanthanide ions are bound by some proteins, it is inevitable that slow exchange obtains in many protein–lanthanide complexes, thereby complicating the ultimate interpretation of the NMR parameters in terms of the geometry of the lanthanide binding site on the protein.

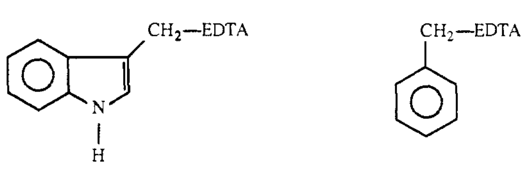

1 2

Figure 1. Indole-EDTA (**1**) and benzyl-EDTA (**2**).

Once the assignments are made, the second step is to determine the elements of the susceptibility tensor of the ion from the pseudocontact shifts. Various assumptions are usually required[18] to separate the contact and the pseudocontact contributions to the LIS of a particular nucleus. These have often involved using theoretical values for magnetic properties of the ions. There is no direct, independent verification of the reliability of these separation procedures. In addition, axial symmetry of the susceptibility tensor was often assumed because it reduces the number of necessary parameters. Such high symmetry does not usually obtain, and the errors introduced by such an assumption are not delineated. In any event, the coordinates of some nuclei in the molecule must be known independently to establish the susceptibility parameters before the LIS values can be used to locate the other nuclei. The third step of calculating the distances from LIR data is essential to obtain the unknown coordinates because the distance and orientation factors are not separable in the LIS expressions as will be discussed below. Finally, since the spherical coordinates of a given nucleus consist of two angular coordinates, experimental data (and elements of the susceptibility tensors) from at least two paramagnetic ions are necessary for a complete determination of the molecular structure. The validity of the procedure rests upon the presumption that the complexes are isostructural, or nearly so, for the lanthanides used.

In an attempt to resolve some of the confusion involved in the application of this method for molecular structure determination, we embarked upon a study of two aromatic derivatives of ethylenediaminetetraacetic acid (EDTA), indole-EDTA and benzyl-EDTA, denoted **1** and **2**, respectively, in Figure 1. Each molecule tightly chelates a single lanthanide ion at the EDTA moiety. They, therefore, serve as models for the interaction of lanthanide ions with aromatic amino acid residues in calcium binding proteins, an extension of our interest in the calcium-activated bioluminescent protein aequorin.[25,26] These EDTA derivatives have also proved to be informative in modeling of fluorescence energy transfer between aromatic fluorophores and Tb and Eu ions.[27–29] The X-ray structure of La^{3+}-EDTA is known[30] and served as a starting point for molecular mechanics calculation of the structures of **1** and **2** which were taken to represent time-averaged solution structures. Proton NMR spectra of **1** and **2** obtained with four different paramagnetic ions (Pr^{3+}, Nd^{3+}, Eu^{3+}, and Yb^{3+}) were analyzed by using the results of the molecular mechanics calculations. In our analysis no assumptions were made regarding the directions of the principal axes or spatial symmetry of the magnetic susceptibility tensor of the ion. Magnetic susceptibility and contact interaction parameters were determined by linear least-squares fits of the LIS values of protons in the molecule to expressions based upon coordinates obtained from the molecular mechanics calculations rather than by the use of theoretical values of the relavent magnetic properties.

---

(8) Solomon, I. *Phys. Rev.* **1955**, *.9*, 559–565.

(9) Bloembergen, N.; Morgan, L. O. *J. Chem. Phys.* **1961**, *34*, 842–850.

(10) McConnell, H. M.; Robertson, R. E. *J. Chem. Phys.* **1958**, *29*, 1361–1365.

(11) Golding, R. M.; Halton, M. P. *Aust. J. Chem.* **1972**, *25*, 2577–2581.

(12) Bleaney, B. *J. Magn. Reson.* **1972**, *8*, 91–100.

(13) Bleaney, B.; Dobson, C. M.; Levine, B. A.; Martin, R. B.; Williams, R. J. P.; Xavier, A. V. *J. Chem. Soc., Chem. Commun.* **1972**, 791–793.

(14) Cramer, R. E.; Dubois, R.; Self, K. *J. Am. Chem. Soc.* **1974**, *96*, 4125–4131.

(15) Dobson, C. M.; Williams, R. J. P.; Xavier, A. V. *J. Chem. Soc., Dalton Trans.* **1973**, 2662–2664.

(16) Levine, B. A.; Williams, R. J. P. *Proc. R. Soc. (London) A* **1975**, *345*, 5–22.

(17) Marinetti, T. D.; Snyder, G. H.; Sykes, B. D. *J. Am. Chem. Soc.* **1975**, *97*, 6562–6570.

(18) Reilley, C. N.; Good, B. W.; Allendoerfer, R. D. *Anal. Chem.* **1976**, *48*, 1446–1458.

(19) Agresti, D. G.; Lenkinski, R. E.; Glickson, J. D. *Biochem. Biophys. Res. Commun.* **1977**, *76*, 711–719.

(20) Reuben, J.; Elgavish, G. A. *J. Magn. Reson.* **1980**, *39*, 421–430.

(21) Babushkina, T. A.; Zolin, V. F.; Koreneva, L. G. *J. Magn. Reson.* **1983**, *52*, 169–181.

(22) Singh, M.; Reynolds, J. J.; Sherry, A. D. *J. Am. Chem. Soc.* **1983**, *105*, 4172–4177.

(23) Peters, J. A.; Nieuwenhuizen, M. S. *J. Magn. Reson.* **1985**, *65*, 417–428.

(24) Asso, M.; Zineddine, H.; Benlian, D. *Int. J. Pep. Pro. Res.* **1986**, *28*, 437–443.

(25) Kemple, M. D.; Ray, B. D.; Jarori, G. K.; Nageswara Rao, B. D.; Prendergast, F. G. *Biochemistry* **1984**, *23*, 4383–4390.

(26) Ray, B. D.; Ho, S.; Kemple, M. D.; Prendergast, F. G.; Nageswara Rao, B. D. *Biochemistry* **1985**, *24*, 4280–4287.

(27) Prendergast, F. G.; Meares, C. F. *Program and Abstracts*, 10th Annual Meeting, American Society of Photobiology, Vancouver, 1982, p 73.

(28) Abusaleh, A.; Meares, C. F. *Photochem. Photobiol.* **1984**, *39*, 763–769.

(29) Engel, L.; Prendergast, F. G., submitted to *Biochemistry*.

(30) Lee, Byungkook The Crystal Structure of the Ethylenediaminetetraacetic Complexes of Lanthanum(III) and Terbium(III). Ph.D. Thesis, Cornell University, 1967.

The overall objectives of this work were (i) to develop a straightforward method containing a minimum number of assumptions for determination of the structure of molecules in solution based upon the effects of paramagnetic lanthanide ions on the NMR properties of the molecules, (ii) to assess the consequences and accuracy of the assumptions that have been made in previously published methods, and (iii) to ascertain the overall utility of the lanthanide technique in molecular structure determination, especially for large molecules.

II. Theory

A. Paramagnetic Lanthanide-Induced Shifts (LIS). The nuclear resonance shifts induced by paramagnetic lanthanide ions in solution are the sum of contact (δ_c) and pseudocontact (δ_{pc}) shifts. The contact contribution is ion and nucleus dependent, but independent of orientation, and is given in the high-temperature approximation by[11]

$$\delta_C = \frac{A\langle S_z\rangle}{\hbar\gamma B_0} = \frac{\mu_B}{3kT}\frac{A}{\gamma\hbar}g_\Lambda(g_\Lambda - 1)J(J+1) \tag{1}$$

where μ_B is the Bohr magneton, k is Boltzmann's constant, T is the temperature in K, A is the hyperfine interaction parameter normally assumed to be ion-independent, γ is the nuclear magnetogyric ratio, g_Λ is the Lande g-factor of the ion, $\hbar J$ is the total angular momentum of the ion, $\hbar$ is Planck's constant, and $\langle S_z\rangle$ is the expectation value of S_z, the component of the spin of the ion along the direction of the applied magnetic field $\mathbf{B}_0$. The pseudocontact shift is given by[12]

$$\delta_{pc} = \frac{-1}{3N\hbar\gamma r^3}\,\mathrm{Tr}\{\underline{\chi} - 3\hat{\mathbf{r}}(\hat{\mathbf{r}}\cdot\underline{\chi})\} \tag{2}$$

where N is the concentration of paramagnetic ions, and $\mathbf{r}\hat{\mathbf{r}}$ is the ion–nucleus vector. $\underline{\chi}$, the magnetic susceptibility tensor of the ion, is taken to be a symmetric tensor. In terms of a polar angle, θ, and an azimuthal angle, ϕ, of $\hat{\mathbf{r}}$ in a coordinate system fixed in the molecule with the ion at the origin, eq 2 becomes

$$\delta_{pc} = \frac{1}{2N\hbar\gamma}(\bar{\chi} - \chi_{zz})\left\langle\frac{(1 - 3\cos^2\theta)}{r^3}\right\rangle + \frac{1}{2N\hbar\gamma}(\chi_{xx} - \chi_{yy}) \times \left\langle\frac{\sin^2\theta\cos 2\phi}{r^3}\right\rangle + \frac{1}{N\hbar\gamma}\chi_{xy}\left\langle\frac{\sin^2\theta\sin 2\phi}{r^3}\right\rangle + \frac{1}{N\hbar\gamma}\chi_{xz}\left\langle\frac{\sin 2\theta\cos\phi}{r^3}\right\rangle + \frac{1}{N\hbar\gamma}\chi_{yz}\left\langle\frac{\sin 2\theta\sin\phi}{r^3}\right\rangle \tag{3}$$

where $\bar{\chi} = (1/3)\mathrm{Tr}\underline{\chi}$ and χ_{xx}, χ_{yy}, χ_{zz}, χ_{xy}, χ_{xz}, and χ_{yz} are the components of $\underline{\chi}$ in the molecule-fixed coordinate system. The brackets $\langle\ \rangle$ represent an average over the molecular motion. δ_{pc} depends only on the anisotropic part of the magnetic susceptibility, given by

$$\underline{\chi}' = \underline{\chi} - \bar{\chi}\mathbf{\Pi} \tag{4}$$

where $\mathbf{\Pi}$ is the identity. If the axes chosen are the principal axes of $\underline{\chi}'$, the final three terms in eq 3 vanish. Furthermore if $\underline{\chi}'$ is axially symmetric, only the first term remains.

It is clear that if the coordinates of at least five nuclei are known, their pseudocontact shifts can be used to find the five components of the traceless part of the susceptibility by a linear least-squares fit of eq 3 to those shift data. The principal values and principal directions of $\underline{\chi}'$ are readily determined by diagonalization. This procedure is central to the analysis presented here and it makes no assumptions regarding either the direction of the principal axes of $\underline{\chi}'$ or its spatial symmetry as was done in numerous other studies (e.g., see ref 15, 16, 18, 20–24). Unless it is known that the molecule has high symmetry, the chosen directions of the principal axes cannot be correct. For the molecules examined here, for example, there is a significant variation of the directions of the principal axes from those initially chosen by relying on approximate molecular symmetry. Furthermore there was a dramatic deviation from axial symmetry. It should also be noted that the procedure used here differs significantly from that used earlier by those[7,14,17,19] who have determined the principal axes of $\underline{\chi}'$ from LIS data. In their methods eq 3 was written in the principal axis system of $\underline{\chi}'$. Then only two susceptibility parameters remain. For a complete fit, the principal directions are varied in the molecule-fixed frame. Three parameters are needed for such a variation bringing the total to five, the same number that is used in this work for the pseudocontact shifts; but their fitting procedure is necessarily nonlinear since a change in direction of the axes requires recalculating the angular functions. In nonlinear fitting procedures, there are always uncertainties regarding whether the true minimum has been found.

A prerequisite for the determination of $\underline{\chi}'$ is the separation of the contributions, δ_c and δ_{pc}, to the total LIS for which a number of approaches[15,18,20–23,31] have been previously used. The temperature dependence of δ_{pc} is that of $\underline{\chi}'$ assuming no substantial change in molecular structure with temperature. If $\underline{\chi}'$ is expanded in a power series in $1/T$, the leading term[12,32,33] is $1/T^2$. In contrast the leading term in δ_c (eq 1) is $1/T$. Attempts to exploit these differences[18] to effect the separation of δ_c and δ_{pc} have not been successful. A major reason is the limited temperature range over which data are usually available, especially for molecules of biological interest. A second approach is to measure LIS values for a given molecule with several different lanthanide ions and to separate δ_{pc} and δ_c by assuming theoretical values for $\langle S_z\rangle$ and for $\underline{\chi}'$. Axial symmetry or the equivalent is often assumed by either neglecting the nonaxial terms[31] or taking the axial and nonaxial parts of $\underline{\chi}'$ to have the same dependence on the paramagnetic ion[22] (see section IVC). Furthermore, the value of A for a given nucleus in the molecule is assumed to be independent of the paramagnetic ion. There is in addition the implicit assumption that the crystalline electric field parameters do not vary from one paramagnetic ion to the next. (One published technique[21] attempts to circumvent this difficulty.) Our approach, which differs from all the above, entails including explicit parameters to account for the contact interaction in the fitting of the total LIS values.

B. Paramagnetic Lanthanide-Induced Relaxation (LIR). The contributions from the contact and dipolar interactions to the LIR are[6,8,9,34–37]

$$T_{1\mathrm{CONTACT}}^{-1} = \frac{2J(J+1)(g_\Lambda - 1)^2A^2}{3\hbar^2}\left(\frac{\tau_e}{1 + \omega_s^2\tau_e^2}\right)$$
$$T_{2\mathrm{CONTACT}}^{-1} = \frac{2J(J+1)(g_\Lambda - 1)^2A^2}{3\hbar^2}\left(\tau_e + \frac{\tau_e}{1 + \omega_s^2\tau_e^2}\right) \tag{5}$$

$$T_{1\mathrm{DIP}}^{-1} = \frac{2J(J+1)\gamma^2g_\Lambda^2\mu_B^2}{15r^6}\left(\frac{3\tau_c}{1 + \omega_I^2\tau_c^2} + \frac{7\tau_c}{1 + \omega_s^2\tau_c^2}\right)$$
$$T_{2\mathrm{DIP}}^{-1} = \frac{J(J+1)\gamma^2g_\Lambda^2\mu_B^2}{15r^6}\left(4\tau_c + \frac{3\tau_c}{1 + \omega_I^2\tau_c^2} + \frac{13\tau_c}{1 + \omega_s^2\tau_c^2}\right) \tag{6}$$

and

$$T_{1\mathrm{CURIE}}^{-1} = \frac{2g_\Lambda^4\mu_B^4\gamma^2J^2(J+1)^2B_0^2}{5r^6(3kT)^2}\left(\frac{3\tau_R}{1 + \omega_I^2\tau_R^2}\right)\left(1 - \frac{r^3\delta_{pc}N}{\bar{\chi}}\right)$$
$$T_{2\mathrm{CURIE}}^{-1} = \frac{g_\Lambda^4\mu_B^4\gamma^2J^2(J+1)^2B_0^2}{r^6(3kT)^2}\left(4\tau_R + \frac{3\tau_R}{1 + \omega_I^2\tau_R^2}\right)\left(1 - \frac{r^3\delta_{pc}N}{\bar{\chi}}\right) \tag{7}$$

---

(31) Shelling, J. G.; Bjornson, M. E.; Hodges, R. S.; Taneja, A. K.; Sykes, B. D. *J. Magn. Reson.* **1984**, *57*, 99–114.

(32) Stout, E. W., Jr.; Gutowsky, H. S. *J. Magn. Reson.* **1976**, *24*, 389–398.

(33) McGarvey, B. R. *J. Magn. Reson.* **1979**, *33*, 445–455.

(34) Bloembergen, N. *J. Chem. Phys.* **1957**, *27*, 572–573.

(35) Bloembergen, N. *J. Chem. Phys.* **1957**, *27*, 595–596.

(36) Gueron, M. *J. Magn. Reson.* **1975**, *19*, 58–66.

(37) Vega, A. J.; Fiat, D. *Mol. Phys.* **1976**, *31*, 347–355.

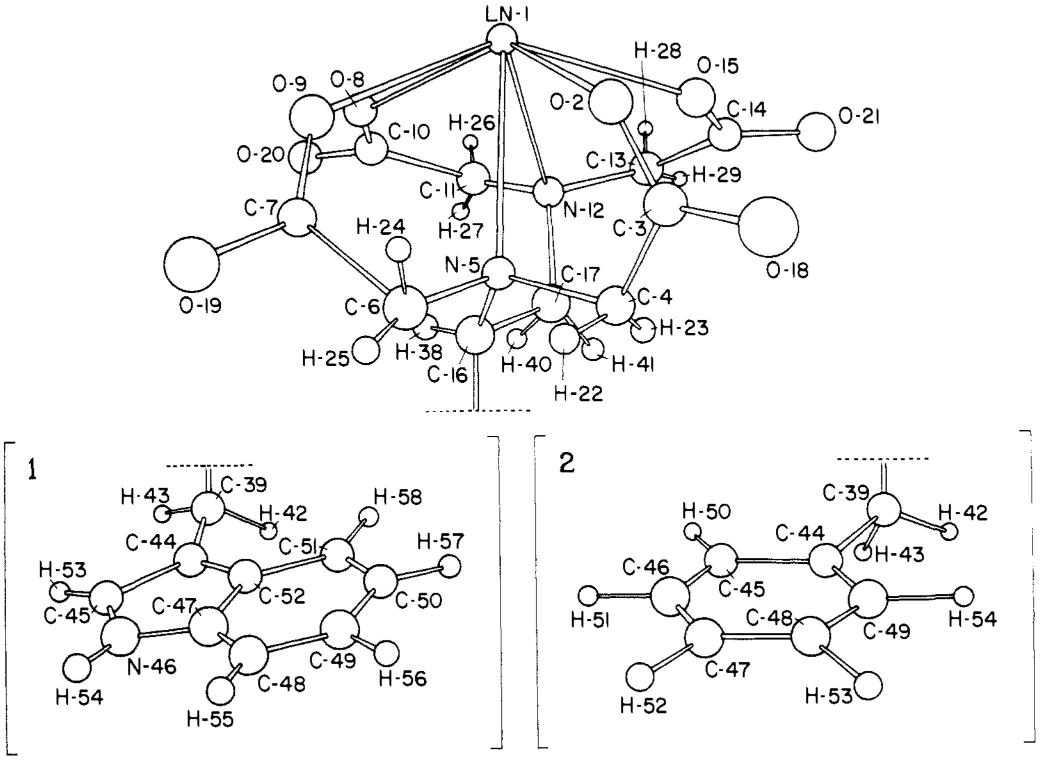

Figure 2. Structure of La-**1** and La-**2** from molecular mechanics calculations showing the atom numbering system used throughout the paper.

where ω_S and ω_I are the angular frequencies for electron and nuclear spin transitions, respectively, in the applied magnetic field, τ_e is the relaxation time of the spin of the paramagnetic ion, τ_R is the rotational correlation time of the molecule, and $\tau_c^{-1} = \tau_e^{-1} + \tau_R^{-1}$. The lifetime of the complex is taken to be long compared with these times. The factor $(g_A - 1)^2$ in eq 5 comes about because the contact interaction is written as $A\mathbf{I}\cdot\mathbf{S}$ where $\mathbf{I}$ and $\mathbf{S}$ are the spin angular momenta of the nucleus and the ion, respectively. The Curie terms, eq 7, arise because the dipolar interaction does not average to zero.

It is generally expected and explicitly shown below that the contact contributions to the LIR (eq 5) are negligible compared with the dipolar terms (eq 6 and 7). The most useful information that comes directly from LIR is the ratio of distances between the nuclei and the ion. It is difficult to obtain actual distances because the correlation times are not usually known with sufficient accuracy. For relatively small molecules such as those examined here the Curie and standard terms are comparable for both T_1^{-1} and T_2^{-1}. For large molecules such as proteins, the Curie term dominates T_2^{-1} and contributes roughly the same[6] as the standard term to T_1^{-1}. Distances can then be calculated from eq 7 for $T_{2\mathrm{CURIE}}^{-1}$ making use of estimates of τ_R from the Stokes-Einstein relationships; τ_e is not needed.

C. Molecular Mechanics. Solution structures for **1** and **2** were calculated by molecular mechanics techniques.[38-40] To determine the most stable structure of **1** and **2**, the MM2 force field was employed[41] because of its reliability and extensive parametrization.[42] However, since MM2 parameters for lanthanum ions do not yet exist,[43] crystallographic data[30] available for La^{3+}-EDTA were used. The crystal data provided atomic coordinates for heavy atoms only. Hydrogens were initially added to the La^{3+}-EDTA complex with use of standard bond lengths and bond angles. In the molecular model, the carboxylate and lanthanum ions were held fixed at the crystallographic coordinates while the remainder of the system including all hydrogens was allowed to fully relax. To search for the most stable conformations, appropriate hydrogens were sequentially replaced by indolyl or benzyl fragments and the most stable orientations of these moieties were located by exhaustively searching all of conformational space with the MM2 dihedral driver options. Multiple minima on the potential energy surface were located. These minima in turn were fully optimized with the crystallographic coordinates of the lanthanide ion bound to the carboxylates being imposed as the only constraint. The most stable structures of **1** and **2** are shown in Figure 2 along with the atom numbering system used throughout this paper. The coordinates of these hydrogens were used in subsequent calculations.

III. Methods and Materials

Indole and 1-benzyl-EDTA were obtained from Dr. Claude Meares (University of California, Davis); their synethesis has been described.[28] The various lanthanide ions used, La^{3+}, Pr^{3+}, Nd^{3+}, Eu^{3+}, Yb^{3+}, and Lu^{3+}, were obtained as chlorides from Alfa-Products. NMR samples were prepared by dissolving either **1** or **2** in D_2O solutions to concentrations of ~5 mM. The pH of the samples was normally adjusted to 7.0 (uncorrected for D_2O in the solvent). The ratio of concentrations of lanthanide ion to **1** or **2** was typically in the range 0.5 to 1.0. These molecules bind one lanthanide ion per molecule at the high affinity typical of EDTA.

The majority of the ^{1}H NMR spectra were obtained with the samples in the temperature range 5–60 °C with a Nicolet (GE) NTC-300 NMR spectrometer equipped with a Nicolet 1280 computer and a 293C pulse programmer. ^{1}H NMR spectra at other frequencies (200 and 470 MHz) were obtained on the corresponding Nicolet NT-200 and NT-470 spec-

---

(38) Boyd, D. B.; Lipkowitz, K. B. *J. Chem. Educ.* **1982**, *59*, 269–274.

(39) Clark, T. *A Handbook of Computational Chemistry: A Practical Guide to Chemical Structure and Energy Calculations*; Wiley-Interscience: New York, 1985; Chapter 2 and reviews cited therein.

(40) Wilson, S. *Chemistry by Computer. An Overview of the Applications of Computers in Chemistry*; Plenum Press: New York, 1986.

(41) Allinger, N. L. *J. Am. Chem. Soc.* 1977, *99*, 8127–8134.

(42) Burkert, U.; Allinger, N. L. *Molecular Mechanics, ACS Monograph 177*; American Chemical Society: Washington, D.C., 1982.

(43) Suitable potentials functions and parameters for metals and organometals do not exist for the MM2 force field and generally are not available for other force fields. These potentials and parameters are chosen to reproduce molecular geometries. Rather than develop an ad-hoc parameter set that may be misleading we decided to use the La^{3+}-EDTA structure directly. Constraining portions of the molecule to its equilibrium geometry while optimizing attached functionality is a common practice (see Chapter 7 of ref 42).

Table I. Chemcial Shift, T_1, and Line Width Values for La-**1**, Pr-**1**, Nd-**1**, and Eu-**1** at 300 MHz and 30 °C[a]

	La-1			Pr-1			Nd-1			Eu-1		
PROTON	δ_d (ppm)	T_1 (s)	line width (Hz)	δ (ppm)	T_1 (s)	line width (Hz)	δ (ppm)	T_1 (s)	line width (Hz)	δ (ppm)	T_1 (s)	line width (Hz)
22	3.81	0.278	2.95	−2.76	0.0756	16.1	2.70	0.0505	42.4	−4.06	0.0902	14.8
23	3.20	0.310	3.30	−12.16	0.0380	26.2	−4.87	0.0183	87.1	−2.90	0.0824	17.8
24	2.94	0.289	3.47	−0.17	0.0524	17.0	6.51	0.0183	39.4	4.23	0.0620	17.0
25	2.94	0.289	3.47	−3.22	0.0447	20.4	6.09	0.0289	17.8	−3.40	0.0924	17.8
26	3.07	0.303	2.78	11.60	0.0347	27.3	5.69		28.6	−3.72	0.0815	19.7
27	3.44	0.338	2.95	5.84	0.0654	12.6	3.96	0.0467	22.1	−6.47	0.0779	17.8
28	3.77	0.276	2.95	9.08	0.0393	15.1	5.15	0.0248	23.6	8.03		19.3
29	3.61	0.364	2.95	1.55	0.0627	21.0	3.01		25.7	1.36	0.0766	17.0
38	3.16	0.305	5.02	−20.02	0.0287	25.9	−12.37	0.0149	94.3	14.32	0.0427	23.7
40	2.66	0.268	3.35	−19.39	0.0292	21.8	−8.97	0.0149	48.7	14.73	0.0412	22.8
41	3.16	0.305	5.02	−6.87	0.0833	17.4	−1.07	0.0446	35.4	−2.84	0.0957	17.0
42	2.41	0.221	4.34	−6.65	0.136	9.5	−2.30	0.0917	21.7	8.35	0.172	12.5
43	2.88	0.248	3.64	−7.83	0.164	12.1	−3.51	0.0990	23.3	8.35	0.172	14.0
53	7.23	1.704	2.39	3.17	0.398	4.6	4.91	0.445	5.9	9.26	1.09	5.2
55	2.53	1.840	3.01	6.43		3.4	6.91	0.829	4.9	8.05		7.3
56	7.26	1.352	4.04	6.53	0.897	3.8	6.87	0.736	4.9	7.64	1.17	8.5
57	7.18	1.349	2.83	6.30	0.798	4.4	6.75	0.589	6.7	7.64	1.17	8.5
58	7.62	1.118	3.05	3.97	0.637	4.8	5.72	0.194	7.4	9.40	0.572	7.3

[a] Blank spaces correspond to unavailable data, either from poor signal-to-noise or spectral overlap.

Table II. Chemical Shift, T_1, and Line Width Values for La-**2**, Pr-**2**, and Yb-**2** at 300 MHz and 30 °C with Selected Chemical Shifts for Lu-**2** Given in Parentheses[a]

	La-2			Pr-2			Yb-2		
PROTON	δ_d (ppm)	T_1 (s)	line width (Hz)	δ (ppm)	T_1 (s)	line width (Hz)	δ (ppm)	T_1 (s)	line width (Hz)
22	3.76	0.326	2.95	−3.22	0.0782	20.0			
23	3.11	0.332	3.30	−12.69	0.0433	27.4			
24	3.02	0.287	3.64	−0.38	0.0572	22.1			
25	3.02	0.287	3.64	−3.42	0.0454	20.8			
26	3.10	0.299	2.95	11.93	0.0337	29.6			
27	3.46	0.387	2.95	6.08	0.0700	17.7			
28	3.60	0.414	2.95	9.04	0.0430	17.0			
29	3.60	0.414	2.95	1.53	0.0654	18.2			
38	3.02	0.287	3.64	−20.60	0.0343	27.3			
40	2.40	0.260	4.94	−19.35	0.0299	27.3			
41	3.02	0.287	3.64	−6.99	0.0902	22.1			
42	2.33 (2.67)	0.231	4.94	−6.86	0.152	12.9	6.26	0.0778	15.5
43	2.85 (2.90)	0.251	5.71	−8.25	0.160	13.7	6.64	0.0791	13.7
50	7.24 (7.26)	1.056	4.38	2.68	0.562	8.5	8.61	0.257	9.2
51	7.39 (7.40)	1.384	4.50	5.61	1.19	7.5	7.91	0.964	7.8
52	7.31 (7.32)	1.556	5.13	5.92	1.40	7.8	7.69	1.15	7.4
53	7.39 (7.40)	1.384	4.50	5.61	1.19	7.5	7.91	0.964	7.8
54	7.24 (7.26)	1.056	4.38	2.68	0.562	8.5	8.61	0.257	9.2

[a] Blank spaces correspond to unavailable data, either from poor signal-to-noise or spectral overlap.

trometers at the Purdue University Biochemical Magnetic Resonance Facility. Both 1D- and 2D-NMR experiments were performed. Proton signals from residual HDO in the D_2O solutions were suppressed by continuous monochromatic radio frequency irradiation during the delay period following data acquisition. All spectra were referenced to 2,2-dimethyl-2-silapentane-5-sulfonate (DSS). T_1 measurements were made by using the standard inversion-recovery sequence with a composite π pulse and either two or three parameter single exponential fits of the signal recoveries. T_2 values were calculated from the line widths. Simulations were used to determine the individual line widths of incompletely resolved doublet and triplet signals. The paramagnetic ion contributions to the chemical shift, spin-lattice relaxation rate, and line width of a given proton in the molecule are determined by subtracting the corresponding values of those quantities obtained with a diamagnetic ion (La^{3+} or Lu^{3+}) bound from those obtained with a paramagnetic ion bound. The effects of complexation are not strongly ion dependent. Variations observed between La^{3+} and Lu^{3+} were small compared with the values of the quantities obtained for the paramagnetic ions. Uncertainties in chemical shift and relaxation measurements were ±0.02 ppm and ±5–10%, respectively.

IV. Results

A. ^{1}H Spectra of Diamagnetic Complexes. All resonances regardless of the lanthanide ion were in slow exchange. The chemical shift (δ_d) values along with the T_1 values and line widths at 30 °C and 300 MHz for La^{3+}-indole-EDTA (La-**1**) are given in Table I. The assignments of the resonances were made with the aid of proton decoupling experiments, 2D-COSY (two-dimensional *J*-correlated spectroscopy) experiments, previous measurements on similar molecules, and the results of analysis of the paramagnetic shifts. The assignments of resonances to the five aromatic protons, 53, 55–58 (see Figure 2), were made consistent with the known chemical shifts for tryptophan resonances. Proton 54 is exchanged with deuterium from the D_2O solution. For the five bridge protons, 38, 40–43, the decoupling experiments left two possible sets of assignments. The set which gave the better fit of the paramagnetic shifts to the susceptibility parameters for Pr^{3+} and Nd^{3+} (see section IV.C.) was chosen. For the eight acetate protons, 22–29, the decoupling experiments related the resonances only in pairs. The matching of shifts to specific protons was also based on fits of the paramagnetic shift data. From Table I it is seen that the range of values of the diamagnetic shifts as well as of T_1 and line widths for these protons is small compared with the corresponding values in the paramagnetic complexes. Thus, the specific choice of the diamagnetic chemical shifts of these eight protons is not critical for the analysis that follows.

The chemical shifts, T_1 values, and line widths at 300 MHz and 30 °C for La^{3+}-benzyl-EDTA (La-**2**) are given in Table II. The assignments of resonances to the aromatic protons, 50–54 (see Figure 2), were unambiguously made on the basis of decoupling experiments. Assignments of resonances to the bridge protons, 38, 40–43, and acetate protons, 22–29, were made similarly to those for La-**1** as described above. There are differences

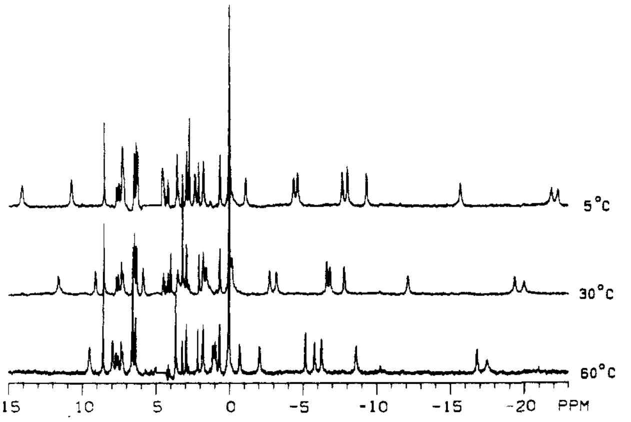

Figure 3. The 300-MHz ^{1}H NMR spectrum of Pr-**1** at 5, 30, and 60 °C. The NMR parameters were the following: pulse length $(\pi/2)$, ~9 μs; spectral width, ±9.1 kHz; data size, 16 K; line broadening, 1 Hz; number of scans, 800 (5 °C) and 1500 (30 and 60 °C).

in the acetate and bridge proton chemical shifts between the two molecules.

The spectrum of Lu-**2** was also measured. It has been suggested that for paramagnetic ions in the first half of the lanthanide group, La^{3+} should be used as the diamagnetic reference, while for those in the second half, Lu^{3+} should serve as the reference.[44] Yb^{3+} is the only ion in the second half of the series used in this study. It was possible to make assignments for only some of the resonances of the Yb^{3+} complexes; therefore, only the corresponding assignments for Lu-**2** are given in Table II. The differences in chemical shifts between La-**2** and Lu-**2** are quite small.

B. ^{1}H Spectra of Paramagnetic Complexes. The assignments of the proton resonances, which were all in slow exchange, were based on (i) proton decoupling experiments, (ii) the structure of the molecules calculated from molecular mechanics, and (iii) T_1 and line width values for the various resonances. The molecular-mechanics structures were utilized to indicate which protons were closer to the paramagnetic ion and therefore should have larger T_1^{-1} and line width values, and often larger shifts. The temperature dependence of the spectra of the paramagnetic complexes allowed overlapping resonances to be separated.

Pr^{3+}-Indole-EDTA and Pr^{3+}-Benzyl-EDTA (Pr-1 and Pr-2). Figure 3 shows the 300-MHz ^{1}H NMR spectrum of Pr-**1** at 5, 30, and 60 °C. Substantial LIS due to the binding of paramagnetic Pr^{3+} and the strong temperature dependence of the LIS are apparent.[45] The chemical shift assignments for Pr-**1** are listed in Table I along with the corresponding T_1 values and line widths obtained at 300 MHz and 30 °C. The acetate protons were coupled in pairs. The final assignments were obtained from the fitting of the shift data (see section IV.C.). The bridge proton lines were assigned by observing from the structure calculations that proton 38 was the nearest to the ion (Table III) and that it should be coupled to both protons 40 and 43 based upon the Karplus relationship[46] applied to the dihedral angles calculated from the structure. Similarly, proton 40 is coupled to 38 and 41 while 43 is coupled to 38 and 42. All of these couplings were observed. In addition, 42 and 43 could be distinguished from 40 and 41 by their longer T_1's and smaller line widths consistent with their larger distances from the ion. In the aromatic part of the spectrum the singlet, 53, was easily assigned. The two doublets, 55 and 58, were distinguished by the fact that the molecular structure showed 58 to be much closer to the ion and therefore it should have a larger shift, smaller T_1, and larger line width. The assignment of the two triplets, 56 and 57, then followed from the decoupling information. The Pr-**2** spectra paralleled the Pr-**1** spectra. Only three aromatic lines were observed in Pr-**2** due to rapid reorientation of the benzyl group. These assignments, 50–54, were made according to the decoupling information and the intensities. The overall assignments, chemical shift, T_1, and line width values at 30 °C and 300 MHz for Pr-**2** are given in Table II. For both of these complexes as the temperature decreased, the LIS for all the protons became larger in magnitude, and the line widths increased.

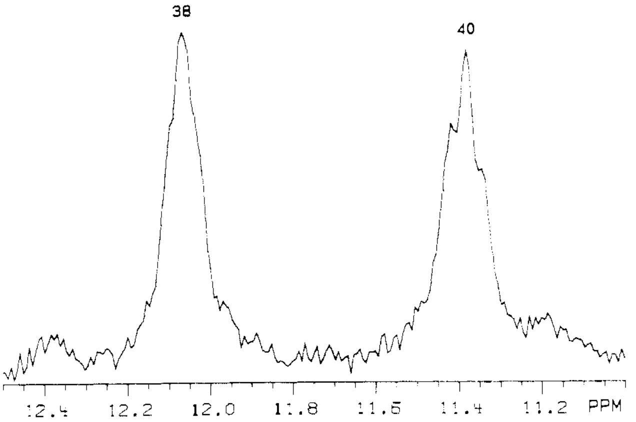

Figure 4. Selected resonances in the 300-MHz ^{1}H NMR spectrum of Eu-**1** at 60 °C. The NMR parameters were the following: pulse length $(\pi/2)$, ~9 μs; spectral width, ±9.1 kHz; data size, 16 K; line broadening, 1 Hz; number of scans, 800.

Nd^{3+}- and Eu^{3+}-Indole-EDTA (Nd-1 and Eu-1). A similar procedure to that just described was followed for making the assignments. Figure 4 gives selected lines of Eu-**1** at 60 °C and clearly illustrates the triplet nature of those lines. The chemical shifts along with T_1 values and line widths at 30 °C and 300 MHz are listed for these ions in Table I. The temperature behavior of the LIS and the line widths of Nd-**1** and Eu-**1** were similar to that of Pr-**1** and Pr-**2**.

Yb^{3+}-Indole-EDTA and Yb^{3+}-Benzyl-EDTA (Yb-1 and Yb-2). Complete assignments could not be made for these complexes because most of the line widths were too large to allow couplings to be resolved. Partial assignments were made for Yb-**2** and are listed in Table II. The chemical shifts are given along with T_1 values and line widths at 30 °C and 300 MHz. The line widths of the proton resonances generally increased as the temperature decreased. The LIS displayed an unusual temperature dependence (see section IV.C.).

C. Analysis. Paramagnetic Shifts. The experimental LIS values for each proton in **1** and **2** for a given paramagnetic ion are given by $\delta - \delta_d$ where δ is the chemical shift value in the presence of the paramagnetic ion and δ_d is the chemical shift of the particular proton in the presence of the diamagnetic ion. Thus the LIS, $\delta - \delta_d = \delta_c + \delta_{pc}$. In eq 3, δ_{pc} for a given proton depends upon the coordinates of that proton in a molecule-fixed frame. Molecule-fixed coordinate systems with the lanthanide at the origin were set up for **1** and **2** from their calculated structures. The structures showed that the ion was located approximately at the center of a nearly planar trapezoid of four oxygen atoms (O-2, O-8, O-9, and O-15 in Figure 2). The z axis of our coordinate system was chosen to pass through the ion, perpendicular to a plane that was least-squares fit to the four oxygens. If, in fact, the ion site did possess fourfold symmetry, the magnetic susceptibility tensor would exhibit axial symmetry about the z axis. The x and y axes were taken to be roughly bisecting the sides of the trapezoid. The polar and azimuthal angles θ and ϕ were then calculated for a vector drawn from the ion to every proton in the molecule in the chosen axis system. The corresponding distances from the ion to the protons were also calculated. The angles and distances are listed in Tables III and IV for **1** and **2**, respectively.

If the δ_{pc} are known from the LIS values, they can be linearly least-squares fit to eq 3 by treating the five quantities $(1/2)(\bar{\chi}$

---

[44] The ionic size decreases from the lighter to the heavier lanthanides (Templeton, D. H.; Dauben, C. H. *J. Am. Chem. Soc.* **1954**, *76*, 5237–5239); thus La^{3+} is expected to be a better reference for the lighter paramagnetic lanthanides and Lu^{3+} for the heavier ones.

[45] The chemical shifts of the protons in the diamagnetic complexes were found to vary by ≤0.03 ppm over the 5–60 °C temperature range so only shifts in the diamagnetic complexes measured at 30 °C were used in subsequent analysis.

[46] Karplus, M. *J. Chem. Phys.* **1959**, *30*, 11–15.

Table III. Molecule-Fixed Coordinates of the Protons of **1** Calculated from the Molecular Mechanics Determined Structure

proton	r (Å)	θ (deg)	ϕ (deg)
22	4.65	31.1	46.3
23	3.85	32.6	4.4
24	3.81	51.3	88.5
25	4.64	35.1	108.7
26	4.04	74.2	253.0
27	4.72	53.7	245.3
28	3.81	77.8	284.1
29	4.72	57.6	290.2
38	3.77	24.8	187.7
40	4.21	28.1	306.9
41	4.77	29.1	262.0
42	5.55	14.3	109.2
43	5.54	8.0	0.3
53	7.15	16.7	273.1
55	9.43	34.8	202.4
56	9.26	43.9	182.6
57	7.63	47.1	165.0
58	5.77	34.4	153.7

Table IV. Molecule-Fixed Coordinates of the Protons of **2** Calculated from the Molecular Mechanics Determined Structure

proton	r (Å)	θ (deg)	ϕ (deg)
22	4.63	30.4	44.8
23	3.80	32.3	2.7
24	3.82	50.8	88.2
25	4.65	34.8	109.0
26	3.90	76.7	252.3
27	4.72	56.2	249.2
28	3.88	77.6	283.9
29	4.72	57.0	289.7
38	3.69	26.8	187.9
40	4.22	27.4	303.7
41	4.74	30.3	259.0
42	5.57	15.1	127.4
43	5.57	4.8	1.2
50	6.26	31.8	174.1
51	8.16	38.0	194.1
52	9.19	34.4	219.1
53	8.66	27.9	247.3
54	6.91	18.4	270.7

$- \chi_{zz})$, $(1/2)(\chi_{xx} - \chi_{yy})$, χ_{xy}, χ_{xz}, and χ_{yz} as fitting parameters. The geometrical factors in eq 3 can be calculated from a set of coordinates for the protons such as those given in Tables III and IV for **1** and **2**. Data from at least five protons must be included. For the majority of the analysis presented here, the 13 aliphatic protons, 22–29, 38, 40–43, were chosen to form the basis. The rationale for excluding the aromatic protons was that (i) the aliphatic protons are closer to the ion and therefore the corresponding δ_{pc} are generally larger leading to greater accuracy in the resulting susceptibility values and (ii) the aromatic moieties are subject to rotation about the bond connecting C-39 and C-44 (Figure 2) and thus their atom-coordinates cannot be precisely specified.

No satisfactory fitting of the data resulted (see below for comparison of such fits with those deemed satisfactory) when the contact shift was neglected for all protons. Introducing contact shift parameters into the fitting procedure requires consideration of the following factors. Unless required by spatial symmetry, each proton in the molecule could have, in principle, a different shift, the details of the contact shift mechanism[47] notwithstanding. On the other hand, no more than eight contact shift parameters may be introduced in order that the total number of fitting parameters (including the five susceptibility parameters) does not exceed the number of LIS values which is 13. Note that the inclusion of δ_c is accomplished by the addition of a geometry-independent parameter to the right-hand side of eq 3 for individual protons. Therefore, fits of the LIS values with reduced overall deviations may result without improving the determination of the susceptibility parameters. In other words, if too many contact parameters are introduced, the flexibility needed for accurate evaluation of the geometry-dependent parameters is lost. In order to avoid this situation either independent criteria for acceptability of the δ_c values must be invoked or a reduction in the number of unconstrained contact shift parameters must be accomplished by using arguments related to the molecular structure. Our approach was the latter. The ultimate affirmation of the procedure rests upon its effectiveness in describing the data and upon the consistency of the results obtained with the various ions at the different temperatures.

There are reasons to expect that the contact shift is negligible for protons several bonds removed from the ion and that it may have nearly the same value for similarly located protons despite the absence of exact spatial symmetry. Each of the eight acetate protons, 22–29, has the same bonding network to the lanthanide ion; thus, similar contact shifts are plausible. Attempts at fits, however, with a single, common contact shift for the acetate protons, but with no contact shift parameters for any other protons, gave unacceptable results. This is not unexpected since the bridge protons, 38, 40, and 41, are the same number of bonds from the La^{3+} (taking N-5 and N-12 to be ligands of the Ln^{3+}) and thus should also have appreciable contact shifts. Reasonable results were obtained for **Pr-1**, **Nd-1**, and **Pr-2**, but not **Eu-1**, when two additional contact shift parameters, one for proton 38, and one for protons 40 and 41, were added to bring the total number of parameters to eight. When yet two more contact shift parameters were added (so that the total number of parameters was ten), acceptable fits for all cases including **Eu-1** were obtained. In particular the acetate protons were divided into two groups, 22–25 and 26–29, and each group was assigned a contact shift parameter. Due to the attachment of the indolyl or benzyl fragment at C-16, there is a basic asymmetry in the molecules, which might lead to differing contact shifts for acetate protons on the two "sides" of the molecules. In addition in these fits separate contact shifts were assigned to each of the three bridge protons. The susceptibility parameters did not change appreciably from the eight to the ten parameter fits for **Pr-1**, **Nd-1**, and **Pr-2**. When further additional contact shifts were assigned to protons 42 and 43, a clear-cut improvement in the fits did not occur.

LIS values from all 18 protons of the molecules (i.e., including the aromatic protons) were also used in some of the analyses. The increased number of data allowed individual contact shifts for each of the acetate protons as well as for the bridge protons to be introduced via fits containing 11 contact shift parameters. These fits amount to using geometrical information only from the remaining seven most distant protons. Consistent results among the various ions were not obtained for (i) the susceptibility parameters, (ii) the sizes of the contact shifts, and (iii) the temperature dependence of the contact shifts from such 16 parameter fits.

In summary the results presented are from linear least-squares fits of LIS values from 13 protons, 22–29, 38, and 40–43, to an expression containing ten parameters (13 × 10 fits). Five of those parameters, common to all protons, represent the pseudocontact interaction (eq 3) while five angle and distance-independent parameters account for the contact interactions, one parameter for protons 22–25, one for protons 23–26, and one each for protons, 38, 40, and 41. Because the nitrogen atoms are directly ligated to the lanthanide ion, it is apparent that the contact interaction is important for protons three bonds removed but negligible for those four bonds removed from the ion in these molecules.

The resonances of the eight acetate protons are known in pairs from the decoupling experiments, and from the T_1 and line width measurements it is generally known which must be the closer of the two protons in each pair. No additional clues are available for making those assignments. Our solution to this problem was a brute-force fitting of the LIS data with all combinations of acetate assignments; the combination that gave the best fit for a given complex was then chosen to represent the correct assignment. That the overall fitting procedure is a valid approach

---

[47] Eaton, D. R.; Phillips, W. D. *Adv. Magn. Reson.* **1965**, *1*, 103–148.

Table V. Magnetic Susceptibility Parameters from 13 × 10 Fits of LIS Values of Protons in Pr-**1**, Nd-**1**, Eu-**1**, and Pr-**2**. Measures of the Quality of the Fits Are Also Included.[a] The Contact Interaction Parameters Are Given in Table VI

	$\xi\chi'_{ww}$ (ppm·Å^3)	$\xi\chi'_{uu}$ (ppm·Å^3)	η	θ_{uz} (deg)	θ_{vz} (deg)	θ_{wz} (deg)	κ (ppm)	AF
Pr-**1**								
(5 °C)	−2112	1797	0.702	94.2	84.2	7.2	1.24	0.026
(30 °C)	−1837	1566	0.704	93.5	84.4	6.6	1.35	0.032
(60 °C)	−1563	1320	0.689	92.4	84.8	5.7	1.55	0.043
Nd-**1**								
(5 °C)	−1520	1499	0.973	101.3	72.6	21.0	1.10	0.039
(30 °C)	−1249	1209	0.936	100.4	73.8	19.4	0.74	0.031
(60 °C)	−981	909	0.854	98.9	75.0	17.5	0.47	0.024
Eu-**1**								
(5 °C)	−2512	1431	0.139	29.3	61.1	94.8	1.67	0.052
(30 °C)	−1850	1012	0.093	11.4	98.3	97.8	0.81	0.031
(60 °C)	−1339	870	0.299	33.4	120.9	101.5	2.07	0.092
Pr-**2**								
(5 °C)	−2242	1962	0.750	92.9	82.5	8.0	1.52	0.031
(30 °C)	−1962	1723	0.756	92.2	82.6	7.8	1.61	0.038
(60 °C)	−1671	1451	0.737	91.2	83.0	7.1	1.77	0.048

[a] The parameters are defined in the text and $\xi = (N\hbar\gamma)^{-1}$. Uncertainties in the susceptibility parameters are ≅10%.

was supported by the facts that (i) the assignment which gave the best fit of the 30 °C data also gave the best fit to the 5 and 60 °C data; (ii) the analogous assignment for Pr-**1** and Pr-**2** gave the best fit for both molecules; (iii) the susceptibility and contact shift parameters generally exhibited the expected decrease with increasing temperature; and (iv) the susceptibility and contact shift parameters were generally consistent among Pr^{3+}, Nd^{3+}, and Eu^{3+} with theoretical expectations.

There were some ambiguities in the assignment of resonances in the diamagnetic complexes. From the decoupling experiments, the acetate proton resonances could only be specified in pairs. In addition two possible sets of assignments of the bridge proton lines were admissible. The problem was resolved by fine tuning the fits of the LIS data. Given a reasonably good fit, the LIS values were varied on the basis of different choices of assignments in the diamagnetic complexes. The assignments giving the best fits were chosen. Those assignments were optimum for Pr-**1** and Nd-**1** at 5, 30, and 60 °C and for the analogous assignments in Pr-**2**. Note that the effects of altering these assignments were small compared with variations resulting from different assignments in the paramagnetically shifted spectra.

The outcomes of the fitting procedure are expressed in terms of the eigenvalues and principal directions, u, v, w, of $\underline{\chi}'$ along with the various contact shift parameters. In particular, χ'_{ww}, χ'_{uu}, η, θ_{uz}, θ_{vz}, and θ_{wz} are given where u, v, and w are chosen such that $|\chi'_{ww}| > |\chi'_{uu}| > |\chi'_{vv}|$, $\eta = (\chi'_{vv} - \chi'_{uu})/\chi'_{ww}$ (an asymmetry parameter, $0 \leq \eta \leq 1$), and θ_{uz}, θ_{vz}, and θ_{wz} are the angles between the u, v, and w axes and the z axis. Angles between the principal directions and the original x and y directions are not listed since the latter directions were essentially arbitrarily chosen. The results of the 13 × 10 fits are given in Tables V and VI for data taken at 5, 30, and 60 °C. All shifts were equally weighted. Two measures of the quality of the fits are listed in Table V,

$$\kappa^2 = [\sum_{j=1}^{13}(\delta_j(\text{meas}) - \delta_j(\text{calc}))^2]^{1/2} \tag{8}$$

and an agreement factor that is often used in these contexts,

$$(\text{AF})^2 = \kappa^2 / \sum_{j=1}^{13}\delta_j^2(\text{meas}) \tag{9}$$

where δ_j represents the total LIS of a given proton. As usual, smaller values of these measures correspond to better fits. The contact shift parameters for protons 22–25, 26–29, 38, 40, and 41 are given in Table VI.

From Table V it is clear that axial symmetry ($\eta = 0$) does not hold for these molecules even though a cursory glance at the ion site in the presumed molecular structure might indicate that it would. Furthermore, there are deviations exceeding the experimental uncertainties of the directions of each of the principal axes of $\underline{\chi}'$ from the initially chosen x, y, and z axes. The directions of the principal axes are not coincident among the ions for the same molecule and additionally show some variation with temperature. The asymmetry parameter varies considerably among the three ions examined.

Table VI. Contact Shifts from 13 ×10 Fits of LIS Values of Protons in Pr-**1**, Nd-**1**, Eu-**1**, and Pr-**2**[a]

	δ_c (ppm)				
ion	protons 22–25	protons 26–29	proton 38	proton 40	proton 41
Pr-**1**					
(5 °C)	3.32 (1.17)	5.13 (1.96)	−3.80 (1.99)	−0.75 (1.93)	3.64 (1.92)
(30 °C)	3.37 (1.27)	3.54 (2.12)	−3.65 (2.15)	−1.57 (2.09)	2.65 (2.08)
(60 °C)	3.37 (1.46)	2.15 (2.43)	−3.14 (2.47)	−2.38 (2.39)	1.88 (2.38)
Nd-**1**					
(5 °C)	5.70 (1.04)	7.31 (1.74)	−9.68 (1.77)	6.42 (1.71)	7.05 (1.70)
(30 °C)	5.35 (0.70)	5.44 (1.17)	−7.39 (1.19)	4.27 (1.15)	5.93 (1.14)
(60 °C)	4.77 (0.44)	3.71 (0.73)	−5.44 (0.75)	2.20 (0.72)	4.85 (0.72)
Eu-**1**					
(5 °C)	−16.54 (1.57)	−13.30 (2.63)	6.51 (2.67)	−1.74 (2.58)	−14.28 (2.57)
(30 °C)	−15.17 (0.76)	−10.47 (1.27)	7.76 (1.29)	−0.49 (1.25)	−12.83 (1.25)
(60 °C)	−14.08 (1.95)	−8.10 (3.26)	8.50 (3.31)	0.80 (3.21)	−11.48 (3.19)
Pr-**2**					
(5 °C)	3.19 (1.49)	6.65 (2.38)	−2.42 (2.43)	1.45 (2.39)	5.58 (2.36)
(30 °C)	3.23 (1.58)	4.94 (2.53)	−2.31 (2.58)	0.48 (2.54)	4.40 (2.50)
(60 °C)	3.23 (1.74)	3.24 (2.78)	−1.97 (2.83)	−0.67 (2.79)	3.27 (2.75)

[a] Standard errors in the parameters based on the fits are given in parentheses.

Table VII. Comparison of Theoretical and Experimental Values of the Primary Principal Value of $\underline{\chi}'$ for Pr-**1**, Nd-**1**, and Eu-**1**.

ion	theory[a]	experiment[b]
Pr^{3+}	1.00	1.00
Nd^{3+}	0.38	0.68
Eu^{3+}	−0.36	−0.55

[a] Bleaney, B. *J. Magn. Reson.* **1972**, *8*, 91–100. Reuben, J.; Elgavish, G. A. *J. Magn. Reson.* **1980**, *39*, 421–430. [b] The experimental values are from 13 × 10 fits of 30 °C LIS data. The principal value of $\underline{\chi}'$ chosen is that with direction nearest the molecule-fixed z axis. Ratios relative to Pr^{3+} are given.

Theoretical calculations[12] give estimates for the ratios of the dominant term in $\underline{\chi}'$ for various lanthanide ions. Table VII gives

Table VIII. Comparison of Theoretical and Experimental Values of the Contact Contribution to the LIS of Protons 22–25, 26–29, 38, 40, and 41 for Pr-**1**, Nd-**1**, and Eu-**1**

		experiment[b]				
ion	theory[a]	protons 22–25	protons 26–29	proton 38	proton 40	proton 41
Pr^{3+}	1.0	1.0	1.0	1.0	1.0	1.0
Nd^{3+}	1.5	1.6	1.5	2.0	-2.7	2.2
Eu^{3+}	-3.6	-4.5	-3.0	-2.1	0.3	-4.8

[a] Ratios of $\langle S_z \rangle$ relative to Pr^{3+} from: Golding, R. M.; Halton, M. P. *Aust. J. Chem.* **1982**, *25*, 2577–2581. [b] The experimental vallues are ratios of the contact interaction parameters relative to Pr^{3+} from 13 × 10 fits of 30 °C LIS data.

a comparison of the theoretical ratios with experimental values derived from the principal values of χ' nearest the z axis. Precise agreement is not expected due to insufficient knowledge of the ion crystal field parameters, to mixing of excited state wave functions into the ground J manifold, to non-colinearity of the principal axes of χ', and to possible deviations in the molecular structures for the different ions.[48]

As mentioned above the contact shifts obtained generally show a decrease in magnitude with increasing temperature (Table VI). Deviations that occur are within the standard errors given by the fitting procedure. It should also be noted that for a given ion complex, the contact shifts do not have the same signs for all of the protons. Sign changes have been observed elsewhere with lanthanides.[49] Contact shift differences between protons 22–25 and 26–29 were greatest for Eu-**1** and of less significance in the other cases. In Table VIII, theoretical estimates[11] of the ratio of contact shifts found with the different ions for protons 22–25, 26–29, 38, 40, and 41 are compared with the contact shifts obtained with **1**. For the theoretical estimates to accurately reflect the shifts, A in eq 1 should be ion independent. Good correspondence of the theoretical and experimental ratios for all but proton 40 is seen. This discrepancy may have arisen from differences in the calculated and actual molecular structures. The T_1 measurements (see below) and the large magnitude of the LIS values of proton 40 suggest that proton 40 is closer to the lanthanide ion than is indicated by the calculated structure.

The statistical parameters, κ and AF (eq 8 and 9), along with σ, where $\sigma^2 = \kappa^2$ divided by the number of degrees of freedom, are compared for various fitting procedures in Table IX. The 13 × 5 fits (no contact shift parameters) and 13 × 8 fits (one contact shift parameter for the acetate protons, one for proton 38, and one for protons 40 and 41 together) discussed above are inferior to the 13 × 10 fits in all cases. Clearly contact shifts must be included in the fitting process. Also in confirmation of the choice of 13 × 10 fits as optimal, a decrease in the quality of fits occurred when the five aromatic protons of **1** or **2** were included in the analysis (18 × 10 fits).

Relaxation Data. If correlation times can be measured or accurately estimated, then proton–ion distances can be calculated from LIR. It is necessary, however, to ascertain the relative strengths of the relaxation processes described in section IIB. One concern is the importance of the contact contributions to the relaxation rates as given by eq 5. From the contact shifts determined above from Pr-**1**, Pr-**2**, and Nd-**1** the strength of the contact contribution relative to the dipolar contribution (eq 6) was estimated[50] to be $T_{1\mathrm{CONTACT}}^{-1}/T_{1\mathrm{DIP}}^{-1} \cong 10^{-3}$ and with a similar ratio for T_2^{-1}. Therefore, the contact contribution to both T_1^{-1} and the line width for Pr^{3+} and Nd^{3+} complexes can be safely neglected. Also at issue is the relative importance of the dipolar and Curie terms, eq 6 and 7, respectively. For large molecules the Curie term dominates the line width but both terms contribute to T_1^{-1}. For molecules of the size of **1** and **2** at the frequencies used here, the two contributions are comparable for both T_1^{-1} and the line width.[51] The dipolar contributions depend upon τ_c where $\tau_c^{-1} = \tau_R^{-1} + \tau_e^{-1}$. Since the ion spin-relaxation time, τ_e, is difficult to determine, the ion–nucleus distance cannot be directly calculated from the LIR in our case. However, if the generally small term involving δ_{pc} in eq 7 is neglected, then both the dipolar and Curie contributions to the LIR are proportional to r^{-6}. Thus, ratios of ion–proton distances can be calculated from the LIR data for different protons. Comparison of ratios of proton–lanthanide distances obtained from the molecular mechanics structure and the LIR is made in Tables X and XI. In general, the agreement is reasonable. The largest discrepancies are for the aromatic protons which in turn have the smallest LIR. These results give a good indication that the structures of the various lanthanide complexes are generally similar.[52] If the structures are substantially different, then such differences must be reflected in the orientations of the ion-nuclear vectors and not their lengths.

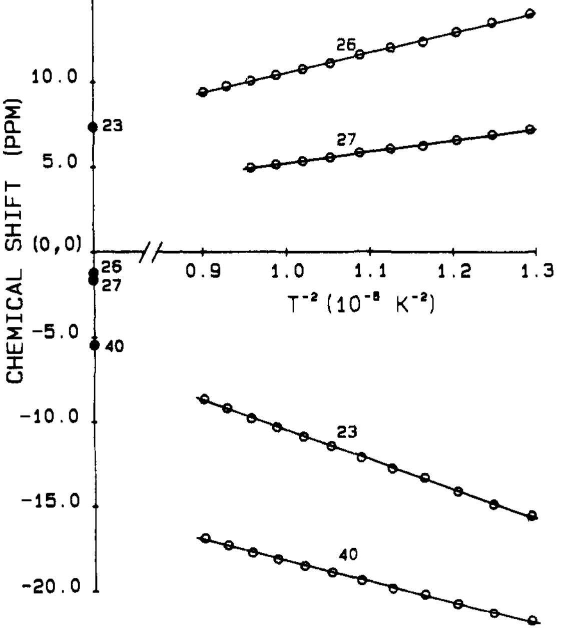

Figure 5. Temperature dependence of the chemical shifts of resonances from protons 23, 26, 27, and 40 in Pr-**1**. Least-squares-fit lines of data to T^{-2} are shown. Values of the shifts, extrapolated to $T^{-2} = 0$, indicated by ● are 7.34, −1.25, −1.66, and −5.45 ppm for protons 23, 26, 27, and 40, respectively.

Temperature Dependence. Both δ_c and δ_{pc} depend on temperature. From eq 3 it can be seen that the temperature dependence

---

(48) Results available in the literature indicate that Ln^{3+} molecular complexes are often essentially isostructural across the Ln series or at least within the respective first and second halves of the series. Sherry et al. (Sherry, A. D.; Yang, P. P.; Morgan, L. O. *J. Am. Chem. Soc.* **1980**, *102*, 5755–5759) showed that there were two groups of isostructural Ln-EDTA complexes, one with the ions Pr^{3+} through Tb^{3+} and another with Dy^{3+} through Yb^{3+}. For further discussion of these points, see e.g.: Bryden, C. C.; Relley, C. N. *Anal. Chem.* **1981**, *53*, 1418–1425. Peters, J. A. *J. Magn. Reson.* **1986**, *68*, 240–251. Yb^{3+} was the only paramagnetic ion from the second half of the series used in this study.

(49) Angyal, S. J.; Littlemore, L.; Gorin, P. A. J. *Aust. J. Chem.* **1985**, *38*, 411–418.

(50) For a given δ_c, A can be calculated from eq 1. For example, if δ_c = 4 ppm = 4×10^{-6} at 30 °C, $A/h = 7.2 \times 10^4$ Hz for Pr^{3+}. To compare the contact and dipolar relaxation strengths, care must be taken with the units. Parameters appearing in the relaxation expressions are usually listed in SI units. To make the dipolar terms, eq 6, and the Curie terms, eq 7, appropriate in SI units, each must be multiplied by $(\mu_0/4\pi)^2$ where $\mu_0 = 4\pi \times 10^{-7}$ N/A^2 is the permeability of free space. The contact term, eq 5, does not require modification. It is difficult to assess the relative importance of the relaxation terms for Eu^{3+} since $J = 0$ in the ground state. However, from the observation of the existence of substantial pseudocontact shifts from Eu-**1** (caused by mixing of excited states with $J \neq 0$) and the ultimate agreement of distances for the various ions, it is likely that the contact contribution to the relaxation is also negligible for Eu^{3+}.

(51) In the study by McLennan and Lenkinski of adriamysin (McLennan, I. J.; Lenkinski, R. E. *J. Am. Chem. Soc.* **1984**, *106*, 6505–6509), a molecule of similar size to those examined here, it was incorrectly concluded that the Curie contribution to the relaxation rates was negligible compared with the dipolar contribution. A numerical mistake was made in estimates of the relative importance of the terms.

(52) Reuben, J.; Elgavish, G. A. *J. Am. Chem. Soc.* **1978**, *100*, 3617–3619.

Table IX. Comparison of the Quality of Fits of LIS Values from Pr-**1**, Nd-**1**, and Eu-**1** Involving Different Numbers of Contact Parameters[a]

	13 × 5			13 × 8			13 × 10			18 × 10[b]		
	κ (ppm)	σ (ppm)	AF	κ (ppm)	σ (ppm)	AF	κ (ppm)	σ (ppm)	AF	κ (ppm)	σ (ppm)	AF
Pr-**1**												
(5 °C)	6.85	2.42	0.143	3.10	1.39	0.065	1.24	0.72	0.026	2.19	0.77	0.045
(30 °C)	6.16	2.18	0.147	3.06	1.37	0.073	1.35	0.78	0.032	2.01	0.71	0.048
(60 °C)	5.66	2.00	0.158	3.24	1.45	0.090	1.55	0.89	0.043	1.93	0.68	0.053
Nd-**1**												
(5 °C)	9.80	3.47	0.348	1.23	0.55	0.044	1.10	0.64	0.039	3.55	1.25	0.125
(30 °C)	8.17	2.89	0.346	1.31	0.59	0.055	0.74	0.43	0.031	2.73	0.96	0.115
(60 °C)	6.74	2.38	0.349	1.85	0.83	0.096	0.47	0.27	0.024	1.90	0.67	0.098
Eu-**1**												
(5 °C)	22.0	7.78	0.685	8.52	3.81	0.265	1.67	0.96	0.052	3.17	1.12	0.098
(30 °C)	20.0	7.06	0.765	8.37	3.74	0.320	0.81	0.47	0.031	2.57	0.91	0.098
(60 °C)	18.6	6.57	0.825	8.64	3.86	0.383	2.07	1.19	0.092	3.10	1.10	0.137

[a] See text for explanation of the procedures and for definitions of κ, σ, and AF. [b] The sums for calculation of the statistical parameters contain 18 terms here.

Table X. Ratios of Proton–Lanthanide Distances for **1** from the Molecular Mechanics Determined Structure and from the LIR[a]

		$r/r(42)$					
		Pr-**1**		Nd-**1**		Eu-**1**	
proton	calcd structure	from T_1	from LW[b]	from T_1	from LW[b]	from T_1	from LW[b]
22	0.84	0.82	0.86	0.86	0.87	0.74	0.94
23	0.69	0.71	0.78	0.71	0.77	0.73	0.91
24	0.69	0.75	0.85	0.71	0.89	0.68	0.92
25	0.84	0.73	0.82	0.77	1.03	0.75	0.91
26	0.73	0.69	0.77		0.94	0.72	0.89
27	0.85	0.78	0.90	0.84	0.98	0.72	0.91
28	0.69	0.71	0.87	0.75	0.97		0.89
29	0.85	0.77	0.81		0.96	0.71	0.91
38	0.68	0.67	0.79	0.68	0.76	0.63	0.87
40	0.76	0.67	0.81	0.68	0.85	0.63	0.87
41	0.86	0.83	0.87	0.83	0.91	0.75	0.94
42	1.00	1.00	1.00	1.00	1.00	1.00	1.00
43	1.00	1.05	0.92	1.01	0.98	0.95	0.96
53	1.29	1.07	1.15	1.25	1.31	1.25	1.20
55	1.70	1.70[c]	1.53	1.46	1.45	1.79[c]	1.11
56	1.67	1.40		1.48	1.64	1.49	1.11
57	1.37	1.33	1.22	1.37	1.28	1.49	1.06
58	1.04	1.27	1.19	1.07	1.26	1.07	1.11

[a] The distances are expressed relative to that of proton 42. LIR-derived distances are from data taken at 30 °C and 300 MHz unless otherwise noted. The corresponding values of T_1^{-1} and the line width obtained in the diamagnetic complex were subtracted from the values measured in the paramagnetic complexes before the ratios were calculated. Blank spaces correspond to unavailable data. [b] Line width. [c] Average of results at 200 and 470 MHz.

Table XI. Ratios of Proton–Lanthanide Distances for **2** from the Molecular Mechanics Determined Structure and from the LIR[a]

		$r/r(42)$			
		Pr-**2**		Yb-**2**	
proton	calcd structure	from T_1	from LW[b]	from T_1	from LW[b]
22	0.83	0.78	0.88		
23	0.68	0.69	0.83		
24	0.69	0.74	0.87		
25	0.83	0.70	0.88		
26	0.70	0.66	0.82		
27	0.85	0.76	0.90		
28	0.70	0.69	0.91		
29	0.85	0.75	0.90		
38	0.66	0.67	0.83		
40	0.76	0.65	0.84		
41	0.85	0.82	0.87		
42	1.00	1.00	1.00	1.00	1.00
43	1.00	1.00	1.00	1.00	1.05
50	1.12	1.18	1.12	1.19	1.14
51	1.47	1.63	1.18	1.73	1.22
52	1.65	1.78	1.20	1.83	1.29
53	1.55	1.63	1.18	1.73	1.22
54	1.24	1.18	1.12	1.19	1.14

[a] The distances are expressed relative to that of proton 42. LIR-derived distances are from data taken at 30 °C and 300 MHz. The corresponding values of T_1^{-1} and the line width obtained in the La-**2** diamagnetic complex were substracted from the values measured in the paramagnetic complexes before the ratios were calculated. Assignments were not made for protons 22–41 of Yb-**2** as discussed in the text so those distances are not listed. [b] Line width.

of δ_{pc} can arise from two sources, the susceptibility (which is related to the electronic states of the ion and their populations) and the average structure. The former gives a dependence[12,32,33] that can be expressed as an infinite series in T^{-1} (leading term is T^{-2}) while the latter should not make a substantial contribution since the average structure of a molecule (large or small) would not be expected to change significantly over the temperature range of these measurements. $\delta = \delta_d + \delta_c + \delta_{pc}$ thus is expressible as a power series in T^{-1} and is apt to have a complex functional dependence[33] at the temperatures available for the LIS measurements. In any event, as $T \rightarrow \infty$, $\delta \rightarrow \delta_d$. The temperature dependence of the LIS has been used to separate δ_c and δ_{pc}[18] and to assign resonances in paramagnetic complexes.[5,53,54] The limited temperature range possible for LIS studies in liquid solution and the infinite series nature of the temperature dependence noted above suggest a priori that such studies might be problematical.

Examples of the temperature dependence of δ from protons with and without contact shifts are given in Figure 5–7. For protons in Pr-**1** and Nd-**1**, $\delta(T)$ is accurately described by a T^{-2} dependence, a contact contribution notwithstanding (Figure 5). Similar results obtained for Pr-**2** (Figure 7). No such simple functional relationship was found for Eu-**1**, but the LIS did decrease in magnitude as T increased. Yb-**1** and Yb-**2** had several lines with an unusual temperature behavior. Some lines were insensitive to temperature in this range similar to observations by Shelling et al.[53] In the examples shown in the figures and others not shown, it was impossible to effect a consistent separation of δ_c and δ_{pc} from the temperature dependencies in agreement with the results of other workers.[18]

There is no straightforward method for assignment of resonances in paramagnetic complexes containing a large number of protons (e.g., proteins) when slow exchange prevails. Use of the temperature dependence of δ was proposed as a method[5,53,54] to obtain values for the diamagnetic shifts and subsequently to make assignments in proteins by extrapolation to infinite T. Since there were other means to assign the resonances in our study, this approach can be examined critically. Extrapolations of various measured shifts to infinite T are shown in Figures 5–7. Comparisons of the extrapolated shifts with δ_d values given in Tables I and II reveal considerable discrepancies. Similar discrepancies were noted for data from protons not shown in the figures. For Yb-**1** and Yb-**2** several lines manifested a temperature behavior

---

(53) Shelling, J. G.; Hofmann, T.; Sykes, B. D. *Can. J. Biochem. Cell Biol.* **1985**, *63*, 992–997.

(54) Lee, L.; Sykes, B. D. *J. Magn. Reson.* **1980**, *41*, 512–514.

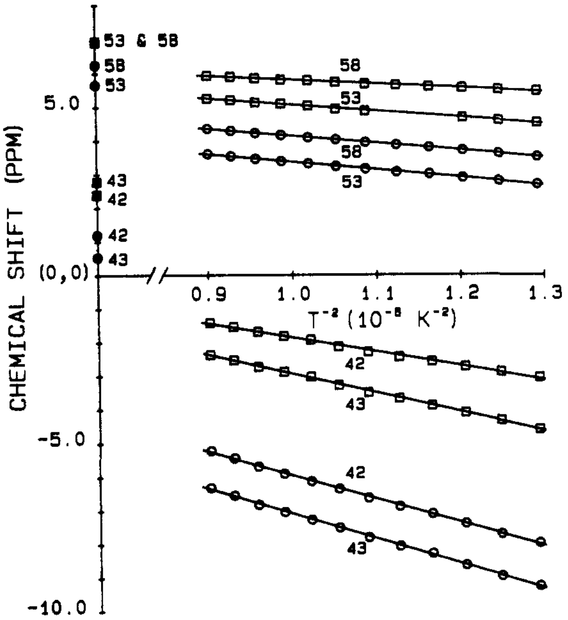

Figure 6. Temperature dependence of the chemical shifts of resonances from protons 42, 43, 53, and 58 in Pr-1 (○) and Nd-1 (□). Least-squares-fit lines of the data to T^{-2} are shown. Values of the shifts, extrapolated to $T^{-2} = 0$, indicated by ● for Pr-1 are 1.19, 0.53, 5.66, and 6.24 ppm and indicated by ■ for Nd-1 are 2.39, 2.78, 6.91, and 6.93 ppm for protons 42, 43, 53, and 58, respectively.

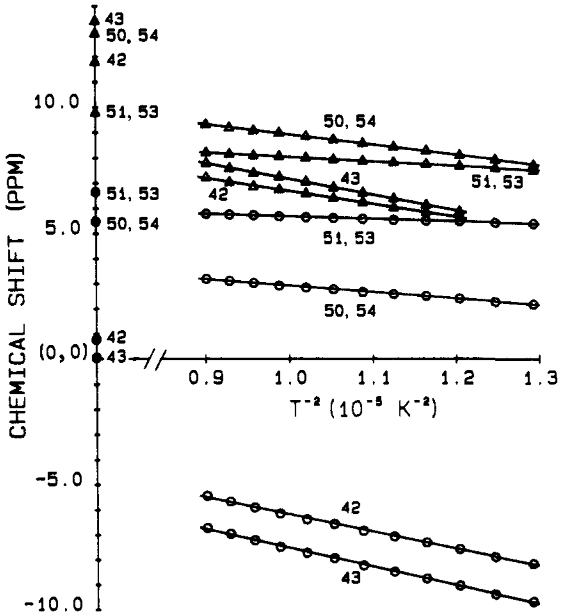

Figure 7. Temperature dependence of the chemical shifts of resonances from protons 42; 43; 51, 53; and 50, 54 in Pr-2 (○) and Yb-2 (▲). Least-squares-fit lines of the data to T^{-2} are shown. Values of shifts, extrapolated to $T^{-2} = 0$, indicated by ● for Pr-2 are 0.77, 0.06, 5.48, and 6.64 ppm and indicated by ▲ for Yb-2 are 11.78, 13.40, 12.90, and 9.77 ppm for protons 42; 43; 51, 53; and 50, 54, respectively.

opposite to that observed from the other ion complexes in that as T increased, δ moved away from δ_d although the dependence was still describable by T^{-2} (see Figure 7 for some examples). If there is an independent notion of the resonance assignments, precise values of δ_d may not be necessary since δ_d is normally small compared with $\delta_c + \delta_{pc}$. However, exclusive use of the temperature dependence of δ for making assignments is not a reliable method. In part, results obtained by extrapolation to infinite temperature are suspect because the limited temperature range of the measurements does not allow precise determination of the functional relationship for $\delta(T)$.

Theoretical Approach To Determine Contact Shifts. Several workers[15,18,20,22,23,31] have attempted separation of δ_c and δ_{pc} by using theoretical values of various ion parameters. For a given ion–nucleus pair, eq 1 and 3 can be combined to give

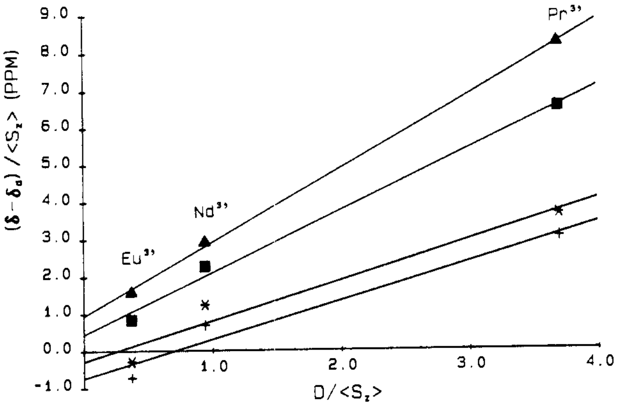

Figure 8. Plots of $(\delta - \delta_d)/\langle S_Z\rangle$ verses $D\langle S_Z\rangle$ for proton 40 at 60 °C (■) and 5 °C (▲) and proton 41 at 60 °C (+) and 5 °C (*). The corresponding contact shifts calculated from the intercepts for 40 and 41 are −1.3 and 2.3 ppm in Pr-1 at 60 °C, −2.7 and 0.9 ppm in Pr-1 at 5 °C; −1.9 and 3.4 ppm in Nd-1 at 60 °C, and −4.1 and 1.4 ppm in Nd-1 at 5 °C; 4.5 and −8.1 ppm in Eu-1 at 60 °C, and 9.8 and −3.2 ppm in Eu-1 at 5 °C.

$$\delta - \delta_d = \delta_c + \delta_{pc} = \frac{A\langle S_z\rangle}{\hbar\gamma B_0} + D\frac{1}{r^3}(1 - 3\cos^2\theta) + E\frac{\sin^2\theta\cos 2\phi}{r^3} \qquad (10)$$

where δ_{pc} is expressed in diagonal form, i.e., in the axis system for which $\underset{\sim}{\chi}'$ is diagonal and the various ion parameters are lumped into D and E. The idea, then, is to measure $\delta - \delta_d$ at a given temperature for a given nucleus in the molecule with different ions. Then for the ith ion eq 10 can be written

$$(\delta - \delta_d)_i = A'\langle S_z\rangle_i + D_iG + E_iF \qquad (11)$$

where $A' = A/\hbar\gamma B_0$, $G = (1/r^3)(1 - 3\cos^2\theta)$, and $F = \sin^2\theta\cos 2\phi/r^3$ are quantities that depend upon the particular nucleus.

Theoretical values are available[11-13,20] for $\langle S_z\rangle_i$ and D_i. These have been used in graphical and numerical procedures to find A' and the geometrical factors with the assumptions that (i) A' is the same for all the ions, (ii) the complexes are isostructural, and (iii) there is effective axial symmetry.[55] For (iii) either axial symmetry is directly assumed by setting $E_i = 0$ for all i in eq 11 or effective axial symmetry is assumed by neglecting the nonaxial terms in eq 11 through geometrical arguments which depend on the details of the molecular structure for their validity, or by supposing that E_i/D_i is independent of i. In other words in the latter case if eq 11 is written as

$$(\delta - \delta_d)_i = A'\langle S_z\rangle_i + D_i\left(G + \frac{E_i}{D_i}F\right) \qquad (12)$$

the factor $G + (E_i/D_i)F$ is taken to be independent of i. The ion independence of E_i/D_i is equivalent to supposing that the ratio of crystal field coefficients,[12] A_{22}/A_{20}, is ion independent. Our results run counter to this assumption. The asymmetry parameter η equals E_i/D_i. As seen in Table V, η varies substantially among the ions used.

Finally, some examples of graphical separation of δ_c and δ_{pc} were attempted with our data under the assumptions described above. As expected since axial symmetry or effective axial symmetry does not apply, satisfactory separations did not result. Neglecting the nonaxial term, eq 11 can be written

$$(\delta - \delta_d)_i/\langle S_z\rangle_i = A' + D_iG/\langle S_z\rangle_i \qquad (13)$$

---

(55) In ref 20 (Reuben, J.; Elgavish, G. A. *J. Magn. Reson.* **1980**, *39*, 421–430), effective axial symmetry was not assumed. They obtained values of E_i that rely to some extent on theoretical values of ion parameters. There is not good agreement between E_i/D_i calculated from ref 20 and η, which equals E_i/D_i, obtained in our study for corresponding ions. Presumably, η is complex specific therefore values obtained for E_i are not of general use.

A plot of $(\delta - \delta_d)/\langle S_z \rangle$ versus $D/\langle S_z \rangle$ can yield a value for A' provided a linear relationship is observed. Our work is limited in that results from only three ions were available for **1**. These ions should satisfy assumption (ii) since they are in the first half of the lanthanide series.[48] Examples are shown in Figure 8 from protons 40 and 41. The intercepts on the vertical axis in Figure 8 for the 5 °C data give the following contact shifts with Pr^{3+}, Nd^{3+}, and Eu^{3+}, respectively: proton 40, −2.7, −4.1, and 9.8 ppm; proton 41, 0.9, 1.4, and −3.2 ppm. These are in very poor numerical agreement with the results of Table VI. Similarly, poor agreement is obtained with the 60 °C data. In fact, an incorrect temperature dependence for the contact shift of proton 41 is predicted. In general, values of the contact shift obtained from the graphical method were found not to be in agreement with our fitted values in Table VI. The assumptions inherent in the graphical method of separating contact and pseudocontact shifts are certainly not met here. When axial symmetry exists, this method of separation is appropriate; otherwise its validity is suspect depending upon the geometrical details.

V. Discussion

We have developed and applied a method of analysis of LIS based upon a linear least-squares fitting procedure incorporating the contact shifts along with the elements of the magnetic susceptibility tensors of the ions as parameters. This work leads us to delineate and scrutinize the methodological tenets involved in using lanthanide ions in NMR determinations of molecular structure in liquid solution. The susceptibility tensor of a paramagnetic ion is dependent on the energy levels and states of the particular ion in the complex. The principal values and directions of $\underline{\chi}'$ will bear no particular relation from one ion to the next even when the complexes are isostructural unless they are constrained by the spatial symmetry of the ion site. In the present work, where at least the Pr-**1** and Nd-**1** complexes, and presumably the Eu-**1** complex, should be expected to be isostructural, the directions of the principal axes of $\underline{\chi}'$ varied considerably. Furthermore axial symmetry cannot be assumed in general. For $\underline{\chi}'$ to have axial symmetry, the lanthanide site must have at least $\bar{3}$-fold symmetry. In some small molecules, intramolecular rotations may lead to an effective time-averaged axial symmetry. Certainly the molecules investigated here did not indicate axial symmetry nor would axial symmetry be expected to obtain for larger molecules of biological interest. Also there is no guarantee that an initial choice of axes based upon approximate symmetry will be the principal axes of $\underline{\chi}'$.

To locate a particular nucleus in the molecule-fixed frame requires three coordinates, such as r, θ, and ϕ. Relaxation data alone are insufficient since T_1^{-1} and the line width have no orientation dependence. Furthermore, because the expression for δ_{pc} (eq 3) contains a sum of terms each in the form of r^{-3} multiplying a function of θ and ϕ the distance cannot be determined from the LIS data independently of the angular factors regardless of the number of ions used. Thus the minimum acceptable information will comprise T_1^{-1} or line width values[56] for finding r, and LIS data from at least two different ions for finding θ and ϕ by iterative solution of eq 3. The iteration is perhaps best accomplished in the principal axis system of $\underline{\chi}'$ since the expression for δ_{pc} reduces to just two terms. Recall, however, that the principal axes are not likely to be coincident for different ions. If the complexes are not isostructural for at least two ions, then, of course, the technique is not appropriate.

In order to follow the above prescription, elements of the susceptibility tensor for the particular ion when bound to the molecule must be found first. Suppose there is no contact contribution to the LIS. Since there are five elements of the susceptibility tensor, the coordinates of at least five nuclei whose resonances are assignable must be known. Some detailed prior knowledge of the molecular structure, e.g., from molecular mechanics calculations or X-ray measurements, is, therefore, imperative. If there is significant contact interaction either for nuclei whose coordinates are presumed to be known or for the nuclei whose coordinates are to be determined, the level of difficulty increases. Some approach for finding δ_c will be necessary. A method that makes exclusive use of either the theoretical parameters of the ion (if there is no axial symmetry) or of the temperature dependence of the LIS does not seem reliable. The procedure used in the present work requires that the coordinates of even more nuclei in the molecule be initially known, depending on the number of contact shift parameters needed. Significant contact interaction was found for protons up to three bonds from the lanthanides Pr^{3+}, Nd^{3+}, and Eu^{3+} in **1** and **2**. As suggested in the literature[5,57] the best ions to use are those that have rather large pseudocontact shifts and relatively small expected contact shifts. These include Yb^{3+}, Tm^{3+}, Pr^{3+}, and Nd^{3+}. Even for Yb^{3+}, it would appear that contact shifts can be safely neglected only for nuclei more than three bonds from the ion. Yb^{3+} evinced somewhat unusual behavior in our study with regard to the temperature dependence of the LIS and excessive line widths which did not allow complete assignment of the resonances. In any event since the LIS method of molecular structure determination depends critically upon structural data from other sources, the results are limited by the accuracy and reliability of those data. Underlying the whole procedure is the task of assigning the resonances to particular nuclei in the molecule which is especially formidable when those resonances are in slow exchange. The key ingredients in this work consisted of information on the scalar coupling network and the molecular geometry. The temperature-dependence measurements of the LIS were useful in resolving resonances that overlapped at a given temperatue, but they were not helpful in making assignments.

The contribution of molecular motion to these structural studies is difficult to ascertain. However, the motion is rapid compared with the observation time of the LIS measurement. Thus structures obtained implicitly represent motional averages. The averaging can, in general, be rather complex owing to the simultaneous presence of multitudinous modes of internal motion. In the case of molecules with ring structures attached through flexible bonds, ring flips are possible. The average of the interaction involves r^{-6} for relaxation and r^{-3} as well as angular factors for shifts. Coordinates obtained are likely to deviate from the equilibrium coordinates.[58-60]

NMR structural techniques using lanthanide ions hold in principle a significant advantage over X-ray methods by allowing the determination of proton coordinates of molecules in liquid solution. We suggest, however, that for macromolecules of biological interest the use of lanthanide methods alone will not readily yield reliable structures. By coupling this method with other approaches such as nuclear Overhauser effect measurements and so-called distance-geometry techniques,[61] one should be able to obtain modestly accurate structures. The LIS are extremely sensitive to the local environment of the paramagnetic ion. Their optimum use for obtaining structures of macromolecules in general and proteins in particular may be in the detection of changes or small differences in structure. For example, when a protein interacts with another molecule or another ion,[62] small changes in the environment of the paramagnetic ion can occur, and these changes can be made quantitative through use of the LIS and LIR data. Furthermore, if metal-binding proteins of suspected similar

---

[56] Between T_1^{-1} and the line width, the former is normally more useful for obtaining ion–nuclear distances since there may be contributions to the line width from other sources. If a single resonance is observed for the bound and free species due to rapid exchange, the lifetimes of the complexes enter the expressions for T_1^{-1} and T_2^{-1}. When the lifetimes are much larger than the relaxation times in the bound complex, the measured relaxation times will not depend on the distances. For details see: Jarori, G. K.; Ray, B. D.; Nageswara Rao, B. D. *Biochemistry* **1985**, *24*, 3487–3494.

[57] Reuben, J. *J. Magn. Reson.* **1973**, *11*, 103–104.

[58] Pedersen, B. *J. Chem. Phys.* **1964**, *41*, 122–132.

[59] Das, T. P. *J. Chem. Phys.* **1957**, *27*, 763–781.

[60] Nageswara Rao, B. D., unpublished calculations.

[61] Havel, T. F.; Kuntz, I. D.; Crippen, G. M. *Bull. Math. Biol.* **1983**, *45*, 665–720.

[62] Shelling, J. G.; Hofmann, T.; Sykes, B. D. *Biochemistry* **1985**, *24*, 2332–2338.

putative structure are examined,[63] small differences in their binding sites may become apparent by comparison of spectra obtained with bound paramagnetic lanthanides. Otherwise, the most fruitful use of lanthanides in proteins would be for determining distances from relaxation measurements, sorting complex NMR spectra by enhancing the resolution, and identifying residues at metal-binding sites. Detailed structures obtained from lanthanide measurements alone must be considered with extreme caution.

Acknowledgment. This work was supported in part by NSF Grants PCM 8022075, DMB 8309120, and DMB 8608185 (B.D.N.R.) and NIH Grant GM 30178 (F.G.P.). Acknowledgment is made to the donors of the Petroleum Research Fund, administered by the American Chemical Society, for partial support of this work (M.D.K.). The NTC-300 NMR spectrometer at IUPUI was purchased with partial support from NSF Grant PCM 8018725. Experiments at 200 and 470 MHz were performed at the Purdue University Biochemical Magnetic Resonance Laboratory which is supported by NIH Grant RR01077 from the Biotechnology Resources Program of the Division of Research Resources. We thank Dr. Claude F. Meares for supplying us with indole- and benzyl-EDTA and Margo Page for processing several versions of this manuscript. The assistance of the following undergraduate students in computer programming and data analysis is acknowledged: Timothy E. Kronenberg, Michael L. Lovejoy, Kimberly J. Redstone, and William T. Stiffler. We also thank the reviewers of this manuscript for their thorough scrutiny and useful suggestions.

---

(63) Lee, L.; Corson, D. C.; Sykes, B. D. *Biophys. J.* **1985**, *47*, 139–142.

Kinetics of Degenerate Rearrangements in Nortricyclyl Cation

Ronald M. Jarret,[*,†] Joseph C. Veniero,[†] Timothy P. Byrne,[†] Martin Saunders,[*,‡] and Keith E. Laidig[‡]

Contribution from the Departments of Chemistry, College of the Holy Cross, Worcester, Massachusetts 01610, and Yale University, New Haven, Connecticut 06511.
Received February 29, 1988

Abstract: Degenerate rearrangements in ^{13}C- and in ^{2}H-labeled nortricyclyl cations are studied with NMR spectroscopy. Label scrambling is detected below 0 °C and results from the combination of three distinct processes. Molecular framework reorganization via the intermediate bicyclo[3.1.1]heptenyl cation, a 3,2-hydride shift (within the norbornenyl cation framework), and a 3,5-hydride shift are the proposed mechanisms responsible for label migration. Changes in the area of NMR signals (^{13}C and ^{2}H) over time at constant temperature are monitored; reaction rates are determined (by the Runge–Kutta method) which accurately simulate these changes. Activation energies of 16.9 ± 1 kcal/mol for the skeletal rearrangement process and 18.4 ± 1 kcal/mol for the 3,2-hydride shift are estimated from the rate data; the activation energy for the 3,5-hydride shift is substantially greater than that of the 3,2-hydride shift. The results from quantum mechanics calculations (MP3/6-31g*//6-31g*) are used to complete the energy profile for the skeletal rearrangement: bicyclo[3.1.1]heptenyl cation is an energy minimum at 5.3 ± 1 kcal/mol, relative to nortricyclyl cation.

The nature of the intermediate carbocation(s) involved in the solvolysis of norbornenyl and nortricyclyl derivatives has been under investigation[1,2] since the early 1950's. Mixtures of norbornenyl and nortricyclyl products are obtained from either type of precursor. Both the symmetric nortricyclyl and asymmetric norbornenyl cations have been postulated[3-7] to explain the observed product distributions. No experimental evidence was found to support the involvement of other proposed intermediates, such as bicyclo[3.1.1]heptenyl cation.[8]

Stable cation solutions have been prepared from both nortricyclyl[9] and norbornenyl[10] halides. Identical NMR spectra are recorded for samples prepared from either alkyl halide, indicating that a common carbocation has been produced. The carbocation appears to be symmetrical on the NMR time scale (^{1}H NMR δ 11.30 (1 H, t), 6.72 (2 H, s), 4.72 (1 H, s), 4.15 (2 H, d), 3.65 (1 H, s), 2.73 (2 H, d); ^{13}C NMR δ 258.5 (d), 111.6 (d), 86.3 (d), 46.6 (t) , 42.4 (d)). Chemical shift additivity[11] is used to identify the compound as the nortricyclyl cation,[9] ruling out the possibility that the observed symmetry is the result of a rapidly equilibrating pair of asymmetric norbornenyl cations. This conclusion is supported by the results[10] obtained from application of the method of isotopic perturbation.[12-14]

Thus, the structure of the common cation produced from nortricyclyl and norbornenyl derivatives is best represented by a single tricyclic species (I) with C_2 symmetry. Theoretical treatments[15] (6-31g//6-31g) and ^{13}C–^{13}C coupling constants[16,17] indicate that the C5–C6 bond (1.36 Å, 59.1 Hz) is shorter (higher % s character) than any other C–C bond (C1–C2 is 1.43 Å), and

---

[†] College of the Holy Cross.

[‡] Yale University.

(1) Winstein, S.; Walborsky, H. M.; Schreiber, K. *J. Am. Chem. Soc.* **1950**, *72*, 5795.

(2) Winstein, S.; Shatavsky, M. *J. Am. Chem. Soc.* **1956**, *78*, 592–597.

(3) Roberts, J. D.; Lee, C. C.; Saunders, W. H. *J. Am. Chem. Soc.* **1955**, *77*, 3034–3037.

(4) Winstein, S.; Kosower, E. M. *J. Am. Chem. Soc.* **1959**, *81*, 4399–4408.

(5) Cristol, S. J.; Morrill, T. C.; Sanchez, R. A. *J. Am. Chem. Soc.* **1966**, *88*, 3087–3091.

(6) Spurlock, L.; Cox, W. *J. Am. Chem. Soc.* **1971**, *93*, 146–151.

(7) Cristol, S. J.; Beimborn, D. A. *J. Am. Chem. Soc.* **1973**, *95*, 3651–3654.

(8) Vogel, P.; Delseth, R.; Quarroz, D. *Helv. Chim. Acta* **1975**, *58*, 508–517.

(9) Olah, G. A.; Liang, G. *J. Am. Chem. Soc.* **1975**, *97*, 1920–1927.

(10) Saunders, M.; Jarret, R. M.; Pramanik, P. *J. Am. Chem. Soc.* **1987**, *109*, 3735–3739.

(11) Schleyer, P. v. R.; Lenoir, D.; Mison, P.; Liang, G.; Prakash, G. K. S.; Olah, G. A. *J. Am. Chem. Soc.* **1980**, *102*, 683–691.

(12) Saunders, M.; Jaffe, M. H.; Vogel, P. *J. Am. Chem. Soc.* **1971**, *93*, 2558–2559.

(13) Saunders, M.; Telkowski, L.; Kates, M. R. *J. Am. Chem. Soc.* **1977**, *99*, 8070–8071.

(14) Jarret, R. M.; Saunders, M. *J. Am. Chem. Soc.* **1987**, *109*, 3366–3369.

(15) Binkley, J. S.; Whiteside, R. A.; Raghavachari, K.; Seeger, R.; DeFrees, D. J.; Schlegel, H. B.; Frisch, M. J.; Pople, J. A.; Kahn, L. R. GAUSSIAN 82, Release A; Carnegie-Mellon University, Pittsburgh, PA, 1982.

(16) Bertrand, R. D.; Grant, D. M.; Allred, E. L.; Hinshaw, J. C.; Strong, A. B. *J. Am. Chem. Soc.* **1972**, *94*, 997–999.

(17) Jonsall, G.; Ahlberg, P. *J. Am. Chem. Soc.* **1986**, *108*, 3819–3824.

0002-7863/88/1510-8287$01.50/0